Journal of Circuits, Systems, and Computers
Vol. 18, No. 8 (2009) 1441–1452

World Scientific
www.worldscientific.com

PHASE INTERVAL VALUE ANALYSIS FOR THE MOTOR IMAGERY TASK IN BCI

JIE LI* and LIQING ZHANG†

Department of Computer Science and Engineering,
Shanghai Jiao Tong University, Dongchuan Road 800,
Shanghai, 200240, China
**lijie1216@sjtu.edu.cn*
†*zhang-lq@cs.sjtu.edu.cn*

In neuroscience, phase is assumed to contain more important information about the neural activity than amplitude. However, the most exploited feature in electroencephalogram (EEG) based brain computer interface (BCI) is the amplitude change, phase has been largely ignored, and only phase locking values (PLV) has been introduced in EEG classification recently. In this paper, we define phase interval value (PIV) to explore the phase information of EEG from a new perspective and propose a computational model based on the ordered Parallel Factors (PARAFAC) algorithm to extract feature from multiway PIV data for single trial EEG classification. Application to the motor imagery task demonstrates that PIV is quite effective for EEG classification, providing significant and discriminative features in spatial and spectral dimension. PIV might become an important new tool in the analysis of EEG phase characteristic, and has the great potential use in BCI.

Keywords: Brain computer interface (BCI); electroencephalogram (EEG); ordered PARAFAC algorithm; phase interval value (PIV); tensor.

1. Introduction

Brain computer interface (BCI) is a system that is designed to translate brain activities into sequences of commands for the computer. BCI provides a communication pathway for people to mentally control machines, and is valuable for those with severe motor disabilities. The most popular sensory signal used for BCI is the scalp-recorded electroencephalogram (EEG), because it is a noninvasive measurement of the brain electrical activity and has a temporal resolution of milliseconds.[1,2] The fundamental of EEG based BCI is to identify changes of brain electrical activities in different mental states and utilize classifying the EEG signals to transmit information.[3,4]

EEG signal includes both amplitude and phase characteristics. Now, in EEG based BCI, the most exploited feature is the amplitude change of EEG signal.[5] A number of algorithms have been developed to capture distinctive features from EEG amplitude information in different mental states, e.g., common spatial pattern

(CSP)[6] and power spectral density (PSD). Currently, CSP is the most successful and widely used algorithm.[7] It detects the spectral discriminations between two classes of tasks by calculating discriminative spatial patterns that maximize the variance of one class and at the same time minimize the variance of the other, wherein the variance of the band-pass filtered EEG signals directly reflects the spectral power of the band frequency. For the classification of two classes of motor imageries, CSP is able to achieve the accuracy above 90%.[6,8,9] PSD is another popular method using amplitude information of EEG signals, which calculates spatially localized power spectral density to obtain the spectral discriminative feature. Phase, instead, has been largely ignored in BCI studies,[10] although it is assumed to contain more important information about the neural activity than amplitude in neuroscience.[11,12] Few studies in BCI community detect the phase change, because there is lack of effective measurement to evaluate the phase change characteristic, and moreover, few computation models have ever been proposed to extract the discriminative features from phase information for EEG classification. To our knowledge, so far, only phase locking values (PLV) have been proposed to characterize the stability of the phase differences between the phases and of two signals, that is, phase synchrony. It was first introduced in EEG by Lachaux *et al.*,[13] and has been used in a variety of studies to explore the dynamic integration of distributed neural networks in the brain.[14–16] Only recently, researchers begun to investigate the usefulness of phase to classify EEG in the framework of BCIs by PLV.[10,17,18] However, it has not been able to acquire comparable performance to the methods based on amplitude information.

In this paper, we define phase interval value (PIV) to measure the degree of phase difference between channels. Different from PLV detecting phase synchrony, PIV explores the phase information of EEG from a new perspective. Referenced to the tensor representation of EEG amplitude information,[19–21] we were inspired to construct the multi-way ($channel \times channel \times frequency \times time\ spices$) PIV data. A computational model based on the ordered Parallel Factors (PARAFAC) algorithm is proposed to extract discriminative feature from multi-way PIV for single trial EEG classification, and then is applied to the motor imagery task. The performance of PIV is compared with CSP, PSD and PLV. Simulation results demonstrate that PIV is quite effective for EEG single trail classification, achieving a comparable performance to CSP which proves to be the most successful algorithm in this context.[7] Furthermore, PIV can supply more significant discriminative spatial and spectral patterns than PLV, which indicates that PLV can be a new tool for analysis of EEG phase characteristic.

2. Background Knowledge

In a BCI system, the subject is required to perform different tasks according to predefined mental control paradigms, and then the subject's intention is conveyed by the induced pattern changes of the recorded EEG. The most commonly used mental

control paradigm in BCI is the motor imagery. This is because the motor imagery produces the attenuation of brain α (8–13 Hz) and β (14–30 Hz) rhythms activity over sensorimotor cortex (ERD: event-related desynchronizations) and depending on the part of the body imagined moving, the amplitude of multichannel EEG signals exhibits distinctive spatial patterns.[22] For example, imagining left hand movement led to the decrease of α and β rhythms' power on the sensorimotor cortex of contralateral rain hemisphere and the increase on the ipsilateral hemisphere, whereas the contrary phenomena occurs during imagining right hand movement.

3. Phase Interval Value (PIV)

In this section, we present the definition of phase interval value (PIV). Different from PLV detecting phase synchrony between channels, PIV measures the degree of the phase difference directly.

Given two signals $x(t)$ and $y(t)$, we calculate their convolutions with a complex wavelet at frequency f, which are written as:

$$\widetilde{\mathrm{X}}(t,f) = a_x(t) \exp\, i(ft + \Phi_x(t))\,, \tag{1}$$

$$\widetilde{\mathrm{Y}}(t,f) = a_y(t) \exp\, i(ft + \Phi_y(t))\,. \tag{2}$$

The PIV between x and y at time t and frequency f across trial e is then defined as follow:

$$\mathrm{PIV}_{(x,y,f,t)} = \frac{1}{n}\sum_{e=1}^{n}\left|\left(\frac{\exp\, i(ft + \Phi_x(t)) + \exp\, i(ft + \Phi_y(t))}{2}\right)\right|, \tag{3}$$

while the PLV is given by:

$$\mathrm{PLV}_{(x,y,f,t)} = \left|\frac{1}{n}\sum_{e=1}^{n}(\exp(i\Delta\Phi(t)))\right|, \tag{4}$$

where the $\Delta\Phi(t)$ is the phase difference $\Phi_x(t) - \Phi_y(t)$.

They could also be calculated in time slices instead of trials,

$$\mathrm{PIV}_{(x,y,f,t)} = \frac{1}{\Delta t f_s}\sum_{t=t-\Delta t/2}^{t+\Delta t/2}\left|\left(\frac{\exp\, i(ft + \Phi_x(t)) + \exp\, i(ft + \Phi_y(t))}{2}\right)\right|, \tag{5}$$

$$\mathrm{PLV}_{(x,y,f,t)} = \left|\frac{1}{\Delta t f_s}\sum_{t=t-\Delta t/2}^{t+\Delta t/2}(\exp(i\Delta\Phi(t)))\right|, \tag{6}$$

where the f_s is the sample rate.

Although PLV and PIV both focus on phase information, there are some significant differences between them. PLV measures the variability of the phase difference. If the phase difference varies little, PLV is close to 1, or close to zero, otherwise. PIV measures the degree of the phase difference directly. If the degree of the phase difference is small, PIV is close to 1, or close to zero, otherwise.

The following example indicates the difference between PIV and PLV. Given two complex signals, $\mathrm{X}(t)$ and $\mathrm{Y}(t)$, as follows:

$$\mathrm{X}(t) = \exp((10t)i) \quad 0 < t \leq 1s\,,$$

$$\mathrm{Y}(t) = \begin{cases} \exp((10t + \pi)i)\,, & 0 < t \leq 0.5s \\ \exp((10t)i)\,, & 0.5s < t \leq 1s \end{cases},$$

the phase difference between them vary from π to $-\pi$ at 0.5 s. Suppose the sample rate is 100 Hz, and the PIV and PLV are both calculated in 100 ms time slices. As illustrated in Fig. 1, PIV can identify the change of phase difference between two signals while PLV cannot detect it.

A further example illustrates the difference of PIV and PLV in real EEG data. It is well known that motor imagery is accompanied by Event Related Desynchronizations (ERD) of EEG within 8–30 Hz frequency band and this phenomenon could be evidently observed at contralateral channels over the centro-parietal lobe, e.g., C3 or C4, when a subject imagines the left or right hand movement.[22] For a typical subject performing hand-movement imagery, we calculate the PIV and PLV between C4 and other channels over centro-parietal lobes in 100 ms time slices at 12 Hz. The changes of PIV and PLV from rest state to motor imagery state are shown in Fig. 2 (in order to give a clear illustration, the changes of PIV and PLV are both averaged in 30 trials). As illustrated in Fig. 2, the PLV of C4 decreases when the subject imagines the left-hand movement, and increases when imagines the right-hand movement, while the PIV gives more information about the changing direction

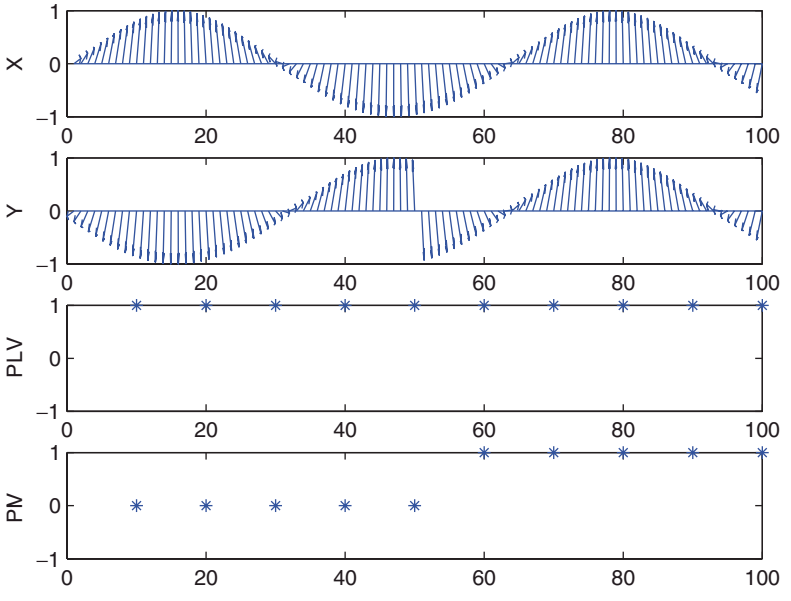

Fig. 1. The feather plots of signals, and PLV, PIV between them.

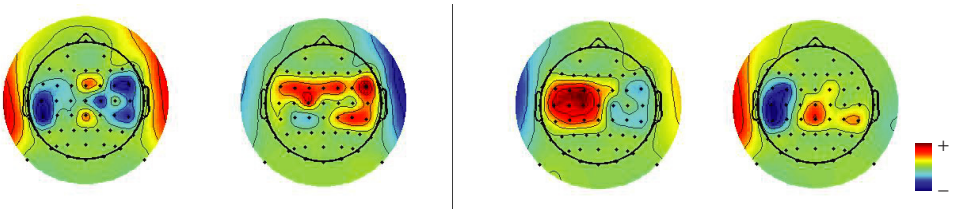

Fig. 2. The left panel shows the change of PLV between C4 and other channels in imagining the left-hand and right-hand movement respectively. The right panel shows the change of PIV between C4 and other channels in imagining the left-hand and right-hand movement respectively.

of phase difference and presents two clear brain regions related respectively with two classes of motor imagery.

4. Method

In this section, we propose a computational model to extract feature from multi-way PIV data for single trial EEG classification and briefly introduce the Ordered PARAFAC algorithm.

4.1. *Computational model*

As illustrated in Fig. 3, the proposed model mainly contains four components: first, 2-way ($channel \times time$) epoched EEG signals $X_{c,t}$ at channel c and time t are decomposed by the wavelet transform and represented as 4-way ($channel \times channel \times frequency \times time$) tensors of $\mathcal{PIV}_{(c_1,c_2,f,t)}$, which denote PIV between channel c_1 and channel c_2 at frequency f and time t. In this work, the complex Morlet wavelet with the center frequency $f_c = 1$ and bandwidth parameter $f_b = 2$ is used as the wavelet mother function, since it has been successfully applied in the analysis of the temporal development of the frequency of EEG signals.[20,21] Secondly, the assemble differences between two classes of PIV in the training dataset are calculated and decomposed into a sum of n rank-one tensors by the ordered PARAFAC algorithm. Lastly, the feature vectors of PIV are obtained by projecting into the subspaces of the rank-one tensors, respectively (here, we can further select several most effective subspaces by the performance in the training dataset and omit others). Finally, a SVM classifier is trained for predicting class label in the test dataset.

4.2. *The ordered PARAFAC algorithm*

A classic PARAFAC model of a m-way tensor $\mathcal{T}$ is to decompose the $\mathcal{T}$ in a minimal sum of n rank-one tensors defined as the outer product of the mode unit vectors,[23]

$$\mathcal{T} = \sum_{r=1}^{n} \left(\prod_{d=1}^{m} \times_d u_r^d \right). \tag{7}$$

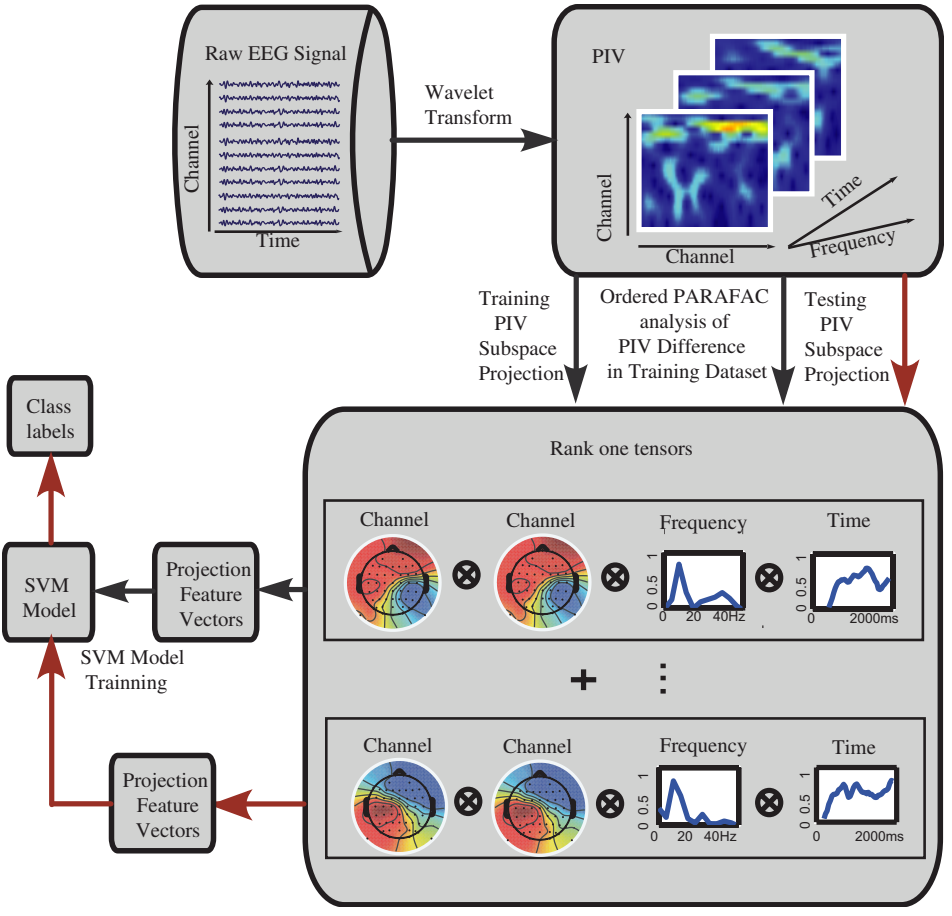

Fig. 3. The proposed computational model to extract feature from multi-way PIV data for single trial EEG classification.

The classical approach of estimating the PARAFAC model is using Alternating Least Squares (ALS) to minimize the reconstruction error,

$$\left\| \mathcal{T} - \sum_{r=1}^{n} \left(\prod_{d=1}^{m} \times_d u_r^d \right) \right\|^2 . \tag{8}$$

While the PARAFAC model is theoretically unique, the decomposed factors are out of order, and the number of factors to be included in the PARAFAC model direct impacts the decomposition.[19] According to our previous work,[24] small changes in the number would lead to great alteration in decomposed factors.

Compared with the PARAFAC Model, the Ordered PARAFAC Model is designed to find a set of rank-one tensors sequentially according to the rule in the algorithm, and the number of factors has no impact on decomposed factors. The Ordered PARAFAC algorithm is implemented as follows: we initialize the ith

rank-one tensor by looking for the first largest component on all modes, then cycle for obtaining the optimal mode vector by remaining fixed the other mode vectors until convergence. After getting the projection coefficients of the $\mathcal{X}$ on the subspace of the ith tensor, we replace $\mathcal{X}$ with its reconstruction error using the ith tensor and the corresponding projection coefficients. This procedure cycles until we get the desired number of the rank-one tensors.

5. Data Acquisition

The dataset was collected during the BCI experiment of motor imagery. Six healthy male subjects, aged from 21 to 30, participated in data collection, and 62 channels of EEG signals were recorded by an ESI-128 Channel High-Resolution EEG/EP Systems (SynAmps2, Neuroscan at Lab for Brian-like Computing and Machine Intelligence, Shanghai Jiao Tong University, China. EEG electrode positioning followed the 10–20 International System of Electrode Placement). In the data collection stage, each subject was asked to seat in an armchair, keeping their arms on the chair arm with two hands relaxed. They were requested to look at a computer monitor placed approximately 1 m in front of the subject (at eye level). They were instructed to imagine the movement of right or left hand for about 2 s to control a cursor movement on the computer screen.

EEG signals were recorded, sampled at 500 Hz, bandpass filtered between 8 Hz and 30 Hz (which contains all α and β rhythms related to motor imagery). Visual inspection showed that artifacts have been mostly filtered out. The filtered signals were segmented into epochs (1–2000 ms) then. For each subject, 100–130 left and 100–130 right trials were acquired, 80 trials (40 trials for each class) were used as training data, and rest trials were taken as test data.

6. Simulations and Results

In this section, the proposed model is applied for single trial EEG classification in the motor imagery task. For comparison, three methods, i.e., CSP, PSD, and PLV, are also applied to the same dataset.

The number of spatial patterns in CSP was selected in 2–8 according to the performance in the training dataset (more patterns would lead to overfitting). For PSD, power spectral density values within 8–30 Hz frequency bands in channel C3 and C4 were computed as feature vectors based on wavelet transform. The four-way PIV tensors ($channel \times channel \times frequency \times time$) were constructed in the given spatial-spatial-spectral-temporal range (62 channel; 62 channel; 8–30 Hz; 1–2000 ms, step by 20 ms). By bootstrapping, it was proven that the 10-factors ordered PARAFAC model was sufficient in this work, and then only two rank-one tensor subspaces were further selected for classification in the training stage. In order to compare the PLV and PIV equally, the construction and application of PLV were the same as PIV. The SVM classifier with the Gaussian Radial Basis (RBF) kernel

Table 1. Simulation results.

Subject	Trial number Train set/Test set	% Classification accuracy PIV	CSP	PSD	PLV
Sub. 1	80/120	90.0	93.3	74.1	60.0
Sub. 2	80/120	66.7	52.5	50.1	42.5
Sub. 3	80/180	88.9	90.6	88.9	63.3
Sub. 4	80/140	59.3	52.1	48.6	54.3
Sub. 5	80/120	66.7	70.8	59.2	50.0
Sub. 6	80/140	45.0	55.0	51.4	51.4

function was determined by a 4-fold cross-validation procedure over the training dataset.

Simulation results of four different methods are listed in the Table 1. For almost all subjects (except Sub. 6), PIV achieved greatly higher accuracies than PLV. For four-sixth of the subjects (Sub. 1, Sub. 2, Sub. 4, Sub. 5), classification accuracies obtained by PIV are higher than PSD. For three of six subjects (Sub. 1, Sub. 3, Sub. 5), PIV achieves very close results to CSP, and especially for two of six subjects (Sub. 2 and Sub. 4), the accuracy of PIV is better than CSP. Considering that CSP is the most successful algorithm in this context,[7] the PIV can be proved to be very effective for EEG classification.

According to Refs. 6 and 22 exemplary spectral characteristics of EEG in motor imagery tasks are α rhythm (8–13 Hz) and β rhythm (14–30 Hz) which decrease during movement or in preparation for movement and increase after movement and during relaxation. In details, imagining left or right hand movement causes ERD over the contralateral hemisphere, and this phenomenon could be evidently observed at contralateral channels over the centro-parietal lobe, e.g., C3 or C4. The two most important projection subspaces for PIV were selected in the training stage. Figures 4 and 5 show the spatial patterns and the spectral patterns of them respectively (because the PIV between channel c_1 and channel c_2 is equal to the PIV between channel c_2 and channel c_1, that is, the spatial patterns are identical

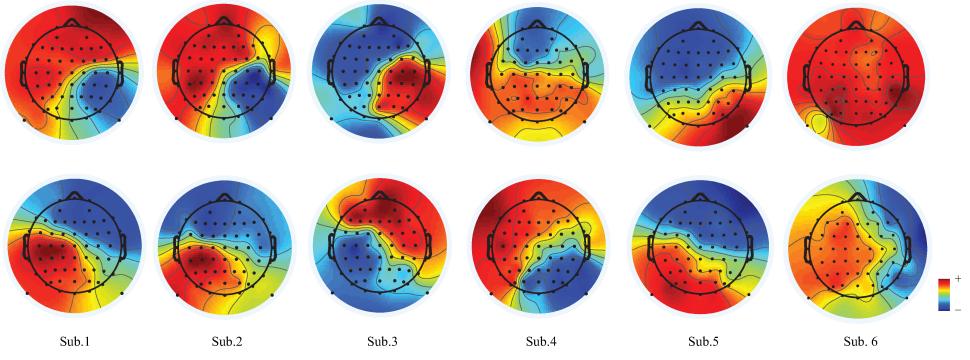

Fig. 4. The two most important spatial patterns of PIV for each subject, respectively.

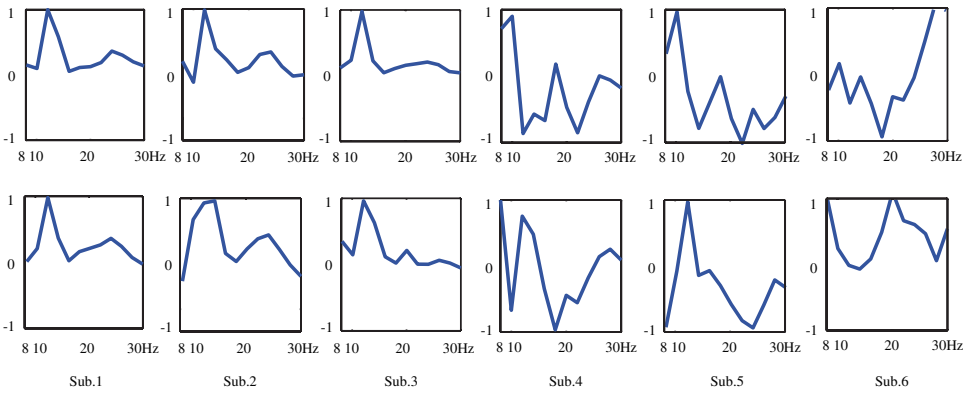

Fig. 5. The two most important spectral patterns of PIV for each subject, respectively.

on two channel-mode, and then we only take one for illustration). Interestingly, the spatial patterns show two regions with opposite weights over the motor-sensor cortex belong to two brain hemispheres (for Sub. 4 and Sub. 6, all methods acquire classification accuracies close to random. Therefore, we ignore them for the pattern analysis). Compared with the spatial patterns of CSP illustrated in Fig. 6, the PIV spatial patterns reflect more clear effects of ERD on contralateral brain hemispheres. The feature vectors of PSD in C3 and C4 channel averaged in the training dataset are also illustrated in Fig. 7, and they (except for Sub. 4 and Sub. 6) are highly consistent with spectral patterns extracted from PIV. The two most important spatial and spectral patterns of PLV are illustrated in Figs. 8 and 9 respectively. For Sub. 1 and Sub. 3, the spatial patterns present some significant regions related with ERD. However, for most of spatial and spectral patterns, it is difficult to identify the motor imagery relevant characteristics.

The results confirm that phase can supply consistent discriminative features with those amplitude information provided. Furthermore, PIV cannot only achieve

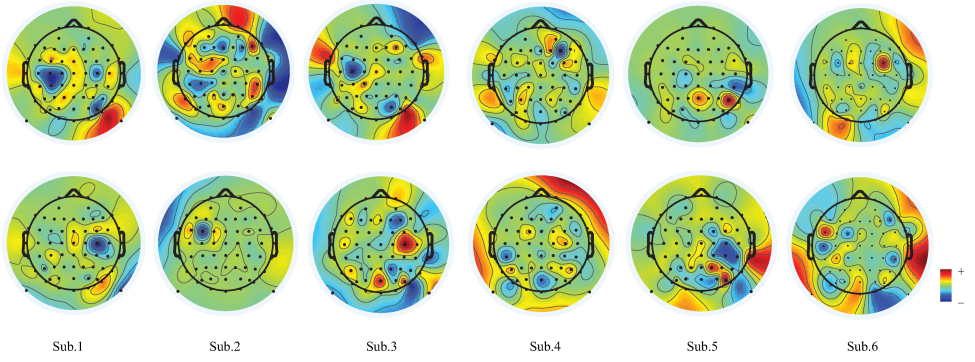

Fig. 6. The two most important spatial patterns extracted by CSP for each subject, respectively.

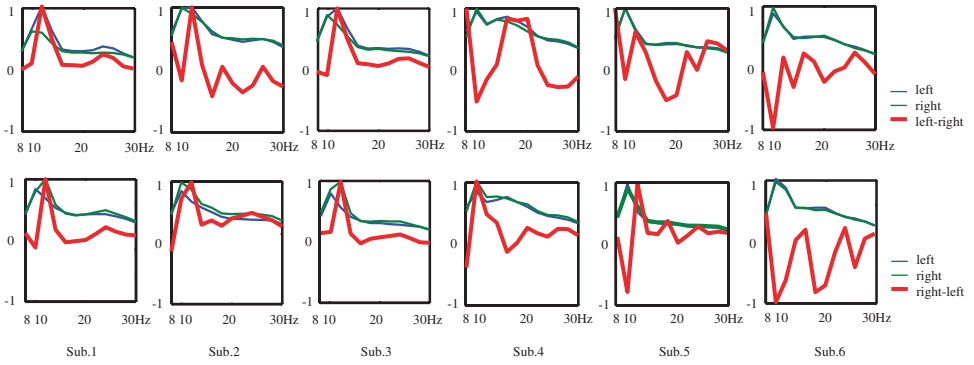

Fig. 7. The feature vectors of PSD in C3 and C4 channel averaged in training dataset for each subject, respectively. The first row is with data recorded in C3, and the second row is with data recorded in C4.

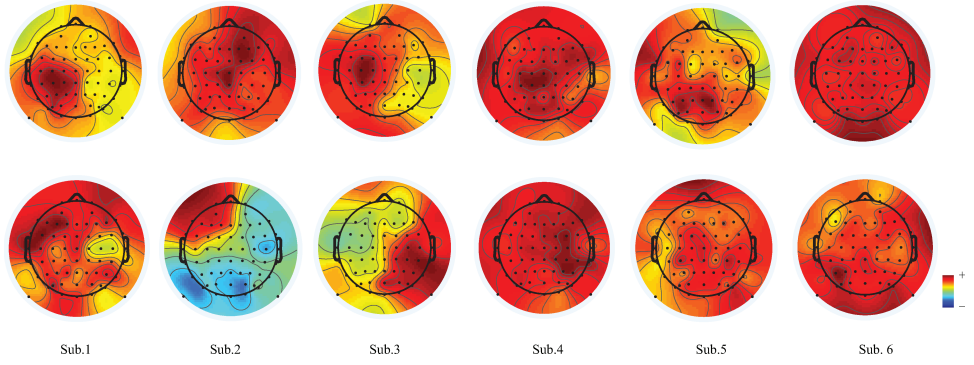

Fig. 8. The two most important spatial patterns of PLV for each subject, respectively.

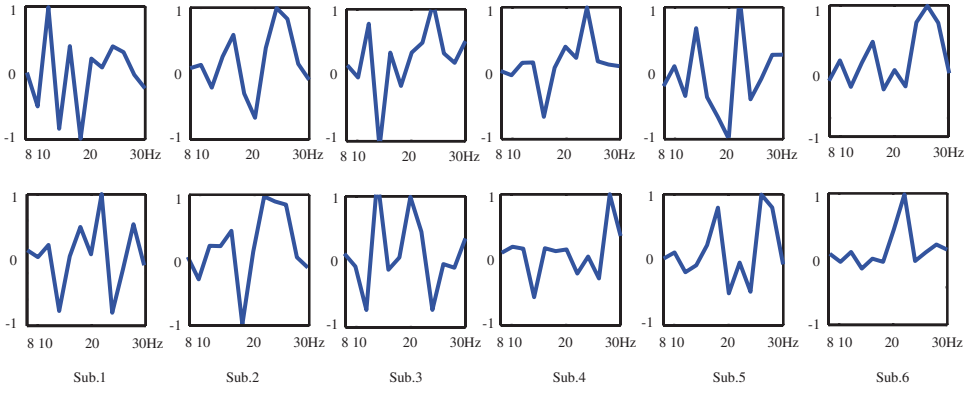

Fig. 9. The two most important spectral patterns of PLV for each subject, respectively.

higher classification accuracy, but also reveal more significant spatial and spectral patterns for discrimination than PLV, though they are both based on phase.

7. Conclusions

In this paper, PIV is defined to further explore the phase information of EEG data from a new perspective, because phase is assumed to contain most important information about the neural activity in neuroscience. A computational model based on the ordered PARAFAC algorithm is proposed to extract feature from multi-way PIV for single trial EEG classification in the motor imagery task.

Simulation results demonstrate that PIV method is very effective for EEG classification, it achieves very close results to CSP, which is the most successful algorithm for EEG classification. It is confirmed that discriminative features could be obtained from phase information. Furthermore, compared with PLV detecting phase synchrony between different channels, PIV can supply more significant spatial and spectral patterns for discrimination by measuring the degree of the phase difference directly.

Since phase information performs so excellently in EEG classification, it is surprising that the phase has been employed so limitedly in BCI studies. PIV might become an important new tool in the analysis of EEG phase characteristic, and has the great potential use in BCI.

Acknowledgments

The authors would like to thank the editors and anonymous reviewers who have given many valuable comments.

The work was supported by the Science and Technology Commission of Shanghai Municipality (Grant No. 08511501701), the National Natural Science Foundation of China (Grant No. 60775007) and the National High-Tech Research Program of China (Grant No. 2006AA01Z125).

References

1. J. R. Millan, F. Renkens, J. Mourino and W. Gerstner, Noninvasive brain-actuated control of a mobile robot by human EEG, *IEEE Trans. Rehabil. Eng.* **51** (2004) 1026–1033.
2. J. R. Wolpaw, N. Birbaumer, D. J. McFarland, G. Pfurtscheller and T. M. Vaughan, Brain-computer interfaces for communication and control, *Clin. Neurophys.* **113** (2002) 767–791.
3. B. Blankertz, G. Curio and K. R. Müller, Classifying single trial EEG: Towards brain computer interfacing, *Advances in Neural Inf. Proc. Systems (NIPS' 01)* **14** (MIT Press, 2002), pp. 157–164.
4. J. R. Wolpaw, N. Birbaumer, W. J. Heetderks, D. J. McFarland, P. H. Peckham, G. Schalk, E. Donchin, L. A. Quatrano, C. J. Robinson and T. M. Vaughan, Brain-computer interface technology: A review of the first international meeting, *IEEE Trans. Rehab. Eng.* **8** (2000) 164–173.

5. F. Lotte, M. Congedo, A. Lécuyer, F. Lamarche and B. Arnaldi, A review of classification algorithms for EEG-based brain-computer interfaces, *J. Neural Eng.* **40** (2007) R1–R13.
6. H. Ramoser, J. Mller-Gerking and G. Pfurtscheller, Optimal spatial filtering of single trial EEG during imagined hand movement, *IEEE Trans. Rehab. Eng.* **8** (2000) 441–446.
7. G. Blanchard and B. Blankertz, BCI competition 2003-data set IIa: Spatial patterns of self-controlled brain rhythm modulations, *IEEE Trans. Biomed. Eng.* **51** (2004) 1062–1066.
8. G. Dornhege, B. Blankertz, G. Curio and K. R. Müuller, Combining features for BCI, *Advances in Neural Inf. Proc. Systems (NIPS'02)* **15** (MIT Press, 2003), pp. 1115–1122.
9. H. Sun and L. Q. Zhang, Subject-adaptive real-time BCI system, *Lecture Notes in Computer Science* **4985** (Springer, 2008), pp. 1037–1046.
10. L. Song, E. Gysels and E. Gordon, Phase synchrony rate for the recognition of motor imagery in BCI, *Advances in Neural Info. Systems (NIPS'05)* **18** (MIT Press, 2006).
11. E. Rodriguez, N. George, J. P. Lachaux, J. Martinerie, B. Renault and F. J. Varela, Perception's shadow: Long-distance synchronization of human brain activity, *Nature* **397** (1999) 391–393.
12. F. Varela, J. P. Lachaux, E. Rodriguez and J. Martinerie, The brainweb: Phase synchronization and large-scale integration, *Nat. Rev. Neurosci.* **2** (2001) 229–239.
13. J. P. Lachaux, E. Rodriguez, J. Martinerie and F. J. Varela, Measuring phase synchrony in brain signals, *Hum. Brain Mapp.* **8** (1999) 194–208.
14. J. Bhattacharya, H. Petsche, U. Feldmann and B. Rescher, EEG gamma-band phase synchronization between posterior and frontal cortex during mental rotation in humans, *Neurosci. Lett.* **311** (2001) 29–32.
15. F. Mormann, T. Kreuz, R. Andrzejak, P. David, K. Lehnertz and C. Elger, Epileptic seizures are preceded by a decrease in synchronization, *Epil. Res.* **53** (2003) 173–185.
16. M. van Putten, Proposed link rates in the human brain, *J. Neurosci. Meth.* **127** (2003) 1–10.
17. E. Gysels and P. Celka, Phase synchronization for the recognition of mental tasks in a brain-computer interface, *IEEE Tran. Neural Syst. Rehab. Eng.* **12** (2004) 406–415.
18. L. Song, Desynchronization network analysis for the recognition of imagined movement in BCIs, *Proc. 27th IEEE EMBS Conference*, Shanghai, China, September 2005.
19. M. Mørup, L. K. Hansen, C. S. Herrmann, J. Parnas and S. M. Arnfred, Parallel factor analysis as an exploratory tool for wavelet transformed event-related EEG, *NeuroImage* **29** (2006) 938–947.
20. M. Mørup, L. K. Hansen, J. Parnas and S. M. Arnfred, Decomposing the time-frequency representation of EEG using non-negative matrix and multi-way factorization, *Technical Reports* (2006).
21. J. Li, L. Q. Zhang, D. C. Tao, H. Sun and Q. B. Zhao, A prior neurophysiologic knowledge free tensor-based scheme for single trial EEG classification, *IEEE Trans. Neural Syst. Rehab. Eng.* **17** (2009) 107–115.
22. G. Pfurtscheller and C. Neuper, Motor imagery activates primary sensorimotor area in humans, *Neurosci. Lett.* **239** (1997) 65–68.
23. R. A. Harshman, Foundations of the PARAFAC procedure: Models and conditions for an "explanatory" multi-modal factor analysis, *UCLA Work Pap. Phon.* **16** (1970) 1–84.
24. J. Li, L. Q. Zhang and Q. B. Zhao, Pattern classification of visual evoked potentials based on parallel factor analysis, *Proc. 1st Int. Conf. Cognitive Neurodynamics*, Shanghai, China, November 2007, pp. 571–575.